

Effect of shear on phase-ordering dynamics with order-parameter-dependent mobility: The large- n limit

N. P. Rapapa

Department of Physics and Astronomy, The University, Manchester M13 9PL, United Kingdom

(Received 28 June 1999)

The effect of shear on the ordering kinetics of a conserved order-parameter system with $O(n)$ symmetry and order-parameter-dependent mobility $\Gamma(\vec{\phi}) \propto (1 - \vec{\phi}^2/n)^\alpha$ is studied analytically within the large- n limit. In the late stage, the structure factor becomes anisotropic and exhibits multiscaling behavior with characteristic length scales $(t^{2\alpha+5}/\ln t)^{1/2(\alpha+2)}$ in the flow direction and $(t/\ln t)^{1/2(\alpha+2)}$ in directions perpendicular to the flow. As in the $\alpha=0$ case, the structure factor in the shear-flow plane has two parallel ridges.

PACS number(s): 64.60.Cn, 82.20.Mj, 05.70.Ln

I. INTRODUCTION

The dynamics of the ordered phases when a system is quenched from the high-temperature phase into the low-temperature region of two or more ordered phases has been of intense interest [1]. It is now well established that in the late stage, both the equal time pair correlation function $C(\mathbf{r}, t)$ and the structure factor $S(\mathbf{k}, t)$ obtained by the Fourier transform of $C(\mathbf{r}, t)$ obey standard scaling. By standard scaling it is meant that $C(\mathbf{r}, t)$ and $S(\mathbf{k}, t)$ can be written as $f(r/L)$ and $L^d g(kL)$, respectively, where $f(r/L)$ and $g(kL)$ are the scaling functions and $L(t)$ is the characteristic length scale in the system. For scaling to hold, $L(t)$ must be well separated from other length scales that may be present in the system. In most of the systems undergoing phase-ordering kinetics, the characteristic length scale $L(t)$ has a power-law dependence on the time t elapsed since the quench, $L(t) \sim t^{1/z}$. The growth exponent z depends on whether or not the order parameter is conserved. In the absence of shear, but with a constant mobility Γ , for nonconserved order parameter systems $z=2$ and for conserved order parameter with no hydrodynamic effects $z=3$ (for scalar fields) and 4 (for vector fields). The characteristic length scale $L(t)$ is normally associated with the wave vector k_m at which the spherically symmetric structure factor $S(\mathbf{k}, t)$ is maximum (i.e., $k_m \sim L^{-1}$).

When the phase-separating system is subjected to uniform shear [2], the isotropy in the structure factor is broken as the domains grow faster in the flow direction than in directions perpendicular to the flow. This anisotropy is confirmed by simulation [3–6] and analytical [7], numerical [8], and experimental results [9–11]. We have previously shown analytically that within the large- n limit [7], the structure factor exhibits multiscaling with characteristic lengths $k_{my}^{-1} = k_{mz}^{-1} \sim (t/\ln t)^{1/4}$ and $k_{mx}^{-1} \sim (t^5/\ln t)^{1/4}$ in directions perpendicular to the flow, and parallel to the flow, respectively. For the scalar case (without hydrodynamic effects), renormalization-group arguments [6] predict $k_{my}^{-1} \sim t^{1/3}$ and $k_{mx}^{-1} \sim t^{4/3}$, for the “viscous hydrodynamic” regime Luger *et al.* [11] found experimentally $k_{my}^{-1} \sim t$ and $k_{mx}^{-1} \sim t^2$. The ratio $k_{mx}^{-1}/k_{my}^{-1} \sim 1/t$ is consistent with analytical, numerical, simulational, and experimental results.

In the case of unsheared phase separation, there has been

much study of the effects of an order-parameter-dependent mobility [12–18]. It was suggested that a mobility of the form $\Gamma(\phi) = 1 - \phi^2$ is appropriate for deep quenches [12] and to account for the effects of external fields such as gravity [13]. Simulational calculations [14] performed on phase separation with scalar order parameter and mobility $\Gamma(\phi) = 1 - a\phi^2$ show that for $a=1$, $z=4$ instead of 3, which is a result for constant mobility. A crossover from $z=4$ to 3 was found for the case where $a < 1$ (with $a > 0$) [14]. For an n -vector order parameter, the simulation results [15] done with $\Gamma(\vec{\phi}) = 1 - a\vec{\phi}^2/n$ for $n=2, 3$, and 4 show a crossover from $z=6$ to $z=4$ for $a < 1$, while for $a=1$, $z=6$. Emmott *et al.* [16,17] considered a more general expression for the mobility given by

$$\Gamma(\vec{\phi}) = \Gamma_0(1 - \vec{\phi}^2/n)^\alpha, \quad (1)$$

where $\alpha \in \mathfrak{R}^+$. For scalar fields [16] in the Lifshitz-Slyozov limit, they found $z=3+\alpha$, while for conserved vector fields within the large- n limit [17] multiscaling was found with two length scales $t^{1/2(\alpha+2)}$ and $k_m^{-1} \sim (t/\ln t)^{1/2(\alpha+2)}$. A different form for the mobility, $\Gamma(\phi) = 1/[1 + \exp(\alpha\phi - \beta\phi^2)]$, where both α and β are positive (with $\beta > \alpha$), was used by Ahluwalia [18] in simulating the Cahn-Hilliard model of phase separation. The domain patterns were found to be similar to the ones observed in viscoelastic phase separation. It is clear that different forms of mobility can be used depending on the type of problem concerned.

Before we proceed, we make few comments on the physical relevance of the parameter α in Eq. (1). For scalar fields (e.g., binary fluids), it is well known that for $\alpha=0$ the bulk diffusion is the dominant coarsening mechanism [1]. When $\alpha > 0$, the bulk diffusion is suppressed since in the bulk phase $\phi^2 \rightarrow 1$ (in dimensionless units) and the mobility Γ vanishes while at the interface $\phi^2 \rightarrow 0$ and Γ is finite leading to surface diffusion (i.e., diffusion along the interfaces). We note that $\alpha=1$ is relevant for deep quenches [12] as noted before, and in simulation one can easily work at zero temperature. For vector fields with $n \leq d$ and constant mobility ($\alpha=0$), there are stable topological defects (e.g., vortex lines for $n=2$ in three dimension) which play the same role as the surfaces (i.e., domain walls) for $n=1$. The coarsening proceeds by a “straightening out” (or a reduction in typical

radius of curvature) as sharp features are removed, or by disappearance of small domain bubbles or vortex loops. For point defects ($n=d$), the coarsening process occurs via the mutual annihilation of defect-antidefect pairs. For $n>d$, there are no stable topological defects and the coarsening dynamics is of a different nature (though the growth exponents may be the same as for $n\leq d$). The analog between the scalar fields and vector fields as far as the coarsening mechanism is concerned in the presence of the order-parameter-dependent mobility is not complete (i.e., it is not clear what are the coarsening mechanisms which correspond to surface and bulk diffusion). It is, however, natural to try to generalize to the vector case [15,17].

In this paper we are mainly concerned with the dynamics of the large- n conserved order parameter with the simplest shear flow following a quench from the high-temperature phase to zero temperature, and the case with an order-parameter-dependent mobility given by Eq. (1). We show that in the late stage, the structure factor becomes anisotropic and shows multiscaling behavior [19] (i.e., $S(\mathbf{k}, t) \sim [(L_x L_y L_z)^{\varphi(k_x L_x, k_y L_y, k_z L_z)}]$ with characteristic length scales $L_x \sim k_{mx}^{-1} \sim (t^{2\alpha+5}/\ln t)^{1/2(\alpha+2)}$, $L_y \sim k_{my}^{-1} \sim (t/\ln t)^{1/2(\alpha+2)}$, and $L_z \sim k_{mz}^{-1} \sim (t/\ln t)^{1/2(\alpha+2)}$ extracted from the maxima of the structure factor. In the $k_z=0$ plane, there are two parallel ridges, whose height and length depend on α . These parallel ridges have been observed in experiments [9] for scalar fields in the absence of shear with $\alpha=0$. It is worth mentioning that multiscaling is believed to be an artifact of the large- n approximation as in the case of constant mobility and zero shear [20]. For systems with finite n , we expect scaling to be recovered asymptotically, although multiscaling may be exhibited as a preasymptotic effect [21].

The paper is organized as follows: In the next section, model equations which take into account both shear and non-constant mobility are introduced. In Sec. III, an exact solution for the structure factor is obtained in the scaling limit. A discussion of the results for specific values of α (i.e., $\alpha=1$ and 2) is presented in Sec. IV. Concluding remarks are given in Sec. V.

II. MODEL EQUATIONS

In order to study the phase-separating system, the Cahn-Hilliard equation (generalized to n -vector order parameter $\vec{\phi}$) is given by

$$\partial_t \vec{\phi} = -\nabla \cdot \{ \Gamma(\vec{\phi}) \nabla [-\nabla^2 \vec{\phi} + \vec{\phi} - (\vec{\phi}^2/n) \vec{\phi}] \}. \quad (2)$$

We are interested in a system with uniform shear flow which has a velocity field of the form $\mathbf{v} = \gamma y \mathbf{e}_x$, where γ is the constant shear rate and \mathbf{e}_x is a unit vector in the flow direction. For an incompressible system in the presence of shear, the term $(\mathbf{v} \cdot \nabla) \vec{\phi}$ is added on the left-hand side of Eq. (2), leading to

$$\partial_t \vec{\phi} + \gamma y \partial_x \vec{\phi} = -\nabla \cdot \{ \Gamma(\vec{\phi}) \nabla [-\nabla^2 \vec{\phi} + \vec{\phi} - (\vec{\phi}^2/n) \vec{\phi}] \}. \quad (3)$$

In the limit $n \rightarrow \infty$, $\vec{\phi}^2/n$ is replaced by its average in the usual way, and Eq. (3) reduces to a linear self-consistent equation whose Fourier transform is given by

$$\frac{\partial \phi_{\mathbf{k}}}{\partial t} - \gamma k_x \frac{\partial \phi_{\mathbf{k}}}{\partial k_y} = -\mathbf{k}^2 a(t)^\alpha [\mathbf{k}^2 - a(t)] \phi_{\mathbf{k}}, \quad (4)$$

where Γ_0 has been absorbed into the time scale, ϕ is (any) one component of $\vec{\phi}$, and $a(t) = 1 - \langle \phi^2 \rangle$. Equation (4) has recently been solved numerically within a ‘‘self-consistent one-loop’’ approximation for a scalar order parameter in two dimensions by Gonnella *et al.* [22]. We believe that the oscillations (whose amplitudes decrease quite rapidly as α increases) found in [22] are slowly decaying preasymptotic transients.

III. EXACT SOLUTION IN THE SCALING LIMIT

Equation (4) is a first-order linear partial differential equation which can be easily solved by change of variables: $(k_x, k_y, t) \rightarrow (k_x, \sigma, \tau)$, with $t = \tau$ and $\sigma = k_y + \alpha k_x \tau$. With this transformation the left-hand side of Eq. (4) becomes $\partial \phi_{\mathbf{k}} / \partial \tau$, and straightforward integration gives (after transforming back to the original variables) $\phi_{\mathbf{k}}(t) = \phi_{\mathbf{k}}(0) \exp f(\mathbf{k}, t)$, where

$$\begin{aligned} f(\mathbf{k}, t) = & -(\kappa^2 + \mu^2)^2 b_0(t) + 4\gamma k_x \mu (\kappa^2 + \mu^2) b_1(t) \\ & - 2\gamma^2 k_x^2 (\kappa^2 + 3\mu^2) b_2(t) + 4\gamma^3 k_x^3 \mu b_3(t) \\ & - \gamma^4 k_x^4 b_4(t) + (\kappa^2 + \mu^2) p_0(t) - 2\gamma k_x \mu p_1(t) \\ & + \gamma^2 k_x^2 p_2(t), \end{aligned} \quad (5)$$

with $\kappa^2 = k_x^2 + k_z^2$, $\mu = k_y + \gamma k_x t$, $b_m(t) = \int_0^t dt' t'^m a(t')^\alpha$, $p_m(t) = \int_0^t dt' t'^m a(t')^{\alpha+1}$.

From dimensional analysis, it is easy to see that to leading order in t , $a(t) \sim t^{-1/(\alpha+2)}$, $L_y \sim L_z \sim t^{1/2(\alpha+2)}$, and $L_x \sim t^{(2\alpha+5)/2(\alpha+2)}$, with the dominant part of the k_x dependence coming from the shear terms. In fact, there are logarithmic corrections to these power-law relations, as we will see. It is reasonable to make the ansatz $a(t) \sim (\ln t/t)^{1/(\alpha+2)}$ (this is true for $\gamma=0$ [17]) in the large- t limit. Then to leading order in t , we have

$$\begin{aligned} b_m(t) &= \frac{2t^m b_0(t)}{m\alpha + 2m + 2}, \\ p_m(t) &= \frac{t^m p_0(t)}{m\alpha + 2m + 1}. \end{aligned} \quad (6)$$

Substituting Eq. (6) into Eq. (5) after making the following change of variables,

$$\gamma k_x = \sqrt{\frac{p_0(t)}{t^2 b_0(t)}} u, \quad k_y = \sqrt{\frac{p_0(t)}{b_0(t)}} v, \quad k_z = \sqrt{\frac{p_0(t)}{b_0(t)}} w, \quad (7)$$

the structure factor $S(\mathbf{k}, t) = \langle \phi_{\mathbf{k}}(t) \phi_{-\mathbf{k}}(t) \rangle$ becomes

$$S(\mathbf{k}, t) = \Delta \exp \left(2 \frac{p_0^2}{b_0} F(u, v, w) \right), \quad (8)$$

$$\begin{aligned}
F(u, v, w) = & -\frac{u^4}{5}A_0(\alpha) - u^3vA_1(\alpha) - 2u^2v^2A_2(\alpha) \\
& - 2uv^3A_3(\alpha) - v^4 + \frac{8}{15}u^2A_5(\alpha) + \frac{4}{3}u vA_4(\alpha) \\
& + v^2 + w^2 - w^4 - 2v^2w^2 - \frac{2}{3}u^2w^2A_2(\alpha) \\
& - 2uvw^2A_3(\alpha),
\end{aligned}$$

where contributions to F which vanish as $t \rightarrow \infty$ (at fixed u, v, w) have been dropped, Δ is the size of the initial fluctuation, $\langle \phi_i(\mathbf{r}, 0) \phi_j(\mathbf{r}', 0) \rangle = \Delta \delta_{ij} \delta(\mathbf{r} - \mathbf{r}')$, and

$$\begin{aligned}
A_0 &= 5 - \frac{40}{\alpha+4} + \frac{60}{2\alpha+6} - \frac{40}{3\alpha+8} + \frac{10}{4\alpha+10}, \\
A_1 &= 4 - \frac{24}{\alpha+4} + \frac{24}{2\alpha+6} - \frac{8}{3\alpha+8}, \\
A_2 &= 3 - \frac{12}{\alpha+4} + \frac{6}{2\alpha+6}, \\
A_3 &= 2 - \frac{4}{\alpha+4}, \\
A_4 &= \frac{3}{2} - \frac{3}{2\alpha+6}, \\
A_5 &= \frac{15}{8} - \frac{30}{8\alpha+24} + \frac{15}{16\alpha+40},
\end{aligned} \tag{9}$$

with $A_m(\alpha=0) = 1$. In order to find the exact form of b_0 and p_0 in the large- t limit, we consider the self-consistent equation for $a(t)$ given by

$$\begin{aligned}
a(t) &= 1 - \int \frac{d^3k}{(2\pi)^3} S(\mathbf{k}, t) \\
&= 1 - \frac{\Delta}{(2\pi)^3 \gamma t} \left(\frac{p_0}{b_0} \right)^{3/2} \\
&\quad \times \int du dv dw \exp\left(2 \frac{p_0^2}{b_0} F(u, v, w) \right). \tag{10}
\end{aligned}$$

The above integral can easily be evaluated by the method of steepest descent using the points of global maxima in $F(u, v, w)$ provided $p_0^2/b_0 \rightarrow \infty$ as $t \rightarrow \infty$ (this is the case we assumed before), therefore Eq. (10) becomes

$$1 = \frac{C_1(\alpha)\Delta}{\gamma t p_0^{3/2}} \exp\left(2 \frac{p_0^2}{b_0} F_m(\alpha) \right), \tag{11}$$

where $C_1(\alpha)$ is a constant and $F_m(\alpha)$ is the value at the maxima $[u_m(\alpha), v_m(\alpha), w_m(\alpha)]$. The assumption that $a(t) \ll 1$ for $t \gg 1$ has also been used.

Therefore, to leading logarithmic accuracy, Eq. (11) leads to

$$\begin{aligned}
p_0^2(t) &\approx \frac{b_0 \ln t}{2F_m} + \frac{3b_0 \ln b_0}{8F_m}, \\
2p_0 \frac{dp_0}{dt} &\approx \frac{db_0}{dt} \left[\frac{\ln t}{2F_m} + \frac{3 \ln b_0}{8F_m} \right]. \tag{12}
\end{aligned}$$

Using Eqs. (12) and the relations $db_0/dt = a^\alpha$, $dp_0/dt = a^{\alpha+1}$, we get

$$a(t) \approx \left(\frac{\ln b_0}{b_0} \right)^{1/2\alpha} \left[\frac{\ln t}{8F_m \ln b_0} + \frac{3}{32F_m} \right]^{1/2}, \tag{13}$$

from which b_0 (since $db_0/dt = a^\alpha$) is found to be

$$b_0(t) \approx \left(\frac{\alpha+2}{2} t \right)^{2(\alpha+2)} \left(\frac{2 \ln t \left[\frac{\alpha+2}{16F_m} + \frac{3}{32F_m} \right]}{\alpha+2} \right)^{\alpha/(\alpha+2)}, \tag{14}$$

from which,

$$\begin{aligned}
\frac{p_0^2(t)}{b_0(t)} &\approx \frac{\ln t}{2F_m} \left[1 + \frac{3}{2(\alpha+2)} \right], \\
a(t) &\approx \left(\frac{4}{(\alpha+2)^2} \frac{\ln t}{t} \right)^{1/(\alpha+2)} \left[\frac{\alpha+2}{16F_m} + \frac{3}{32F_m} \right]^{1/(\alpha+2)}. \tag{15}
\end{aligned}$$

The above results for $a(t)$, $b_0(t)$, and $p_0(t)$ justify our original ansatz. From Eq. (7) we can define the characteristic length scales in three directions: $L_x = \gamma(t^2 b_0/p_0)^{1/2} \sim Y(\alpha) \gamma(t^{2\alpha+5}/\ln t)^{1/2(\alpha+2)}$ and $L_y = L_z = (b_0/p_0)^{1/2} \sim Y(\alpha)(t/\ln t)^{1/2(\alpha+2)}$, by setting $u = k_x L_x$, $v = k_y L_y$, and $w = k_z L_z$, where

$$Y^{-1}(\alpha) = \sqrt{2} \left(\frac{4}{(\alpha+2)^2} \left[\frac{\alpha+2}{16F_m} + \frac{3}{32F_m} \right] \right)^{1/2(\alpha+2)}. \tag{16}$$

Exact values for $F_m(\alpha)$ and $[u_m(\alpha), v_m(\alpha), w_m(\alpha)]$ can be found by specifying values of α . For example, values for $\alpha=1$ and 2 are shown in Table I, while for $\alpha=0$, results presented in [7] are recovered.

Using Eqs. (8), (11), and (15), it is easy to show that the structure factor becomes

$$S(\mathbf{k}, t) = \text{const} [\ln V_s]^{3/2} V_s^{F(\mathbf{q})/F_m}, \tag{17}$$

with scaled momentum \mathbf{q} and ‘‘scale volume’’ V_s given by

$$\mathbf{q} = (k_x L_x, k_y L_y, k_z L_z), \tag{18}$$

$$V_s = L_x L_y L_z \sim \gamma t^{(7+2\alpha)/2(\alpha+2)} (\ln t)^{3/2(\alpha+2)},$$

respectively. Equation (17) exhibits multiscaling behavior (i.e., the power of the ‘‘scale volume’’ depends continuously on the scaling variables). We anticipate, however, that for finite n , standard scaling will be recovered and the $\ln t$ terms (which appear in the characteristic length scales) will be absent as has been shown explicitly for the case with both α and $\gamma=0$ [20].

TABLE I. Stationary points of $F(u, v, w)$: Max=maximum, Min=minimum, S =saddle point (2D), S_n = saddle point of type n (the matrix of second derivatives has n positive eigenvalues), IS=“inflection saddle point” (one positive, one zero, one negative eigenvalue), IMax=“inflection maximum” (one zero, one negative eigenvalue). See also Fig. 1. for 2D results.

Position (u, v, w)	Number	F	Value	Type (3D)	Type (2D)
$\alpha=1$					
(0,0,0)	1	0	0	Min	Min
$\pm(\sqrt{55/6}/3, 0, 0)$	2	55/168	0.32738	IS	IMax
$\pm[(33-\sqrt{165})/18\sqrt{2}, -1/\sqrt{2}, 0]$	2	$31/168 - \sqrt{55/3}/28$	0.03160	S_2	S
$\pm[(33+\sqrt{165})/18\sqrt{2}, -1/\sqrt{2}, 0]$	2	$31/168 + \sqrt{55/3}/28$	0.33744	S_1	Max
$\pm(0, 0, 1/\sqrt{2})$	2	1/4	0.25	S_1	
$\pm(\sqrt{22}/3, -\sqrt{11}/4, \pm\sqrt{5}/4)$	4	39/112	0.34821	Max	
$\alpha=2$					
(0,0,0)	1	0	0	Min	Min
$\pm(\sqrt{7/8}, 0, 0)$	2	14/45	0.31111	IS	IMax
$\pm[(7-\sqrt{7})/4\sqrt{2}, -1/\sqrt{2}, 0]$	2	$31/180 - \sqrt{7}/18$	0.02524	S_2	S
$\pm[(7+\sqrt{7})/4\sqrt{2}, -1/\sqrt{2}, 0]$	2	$31/180 + \sqrt{7}/18$	0.31921	S_1	Max
$\pm(0, 0, 1/\sqrt{2})$	2	1/4	0.25	S_1	
$\pm(\sqrt{35}/4, -\sqrt{7}/5/2, \pm\sqrt{3}/5/2)$	4	59/180	0.32778	Max	

IV. RESULTS

Both the positions of the stationary points of $F(u, v, w)$ and its value depend on α [apart from points (0,0,0) and $\pm(0, 0, 1/\sqrt{2})$], see Table I. The global picture of $S(\mathbf{k}, t)$ is determined by $F(u, v, w)$ [i.e., the stationary points and their type together with values of $F(u, v, w)$ at stationary points] because $\ln S(\mathbf{k}, t) = [F(u, v, w)/F_m] \ln V_s$ (plus \mathbf{k} -independent terms). The features of $F(u, v, w)$ for $\alpha=1$ and 2 are summarized in Table I and Table II.

The parallel ridges found in Fig. 1 are similar to ones found in experiments [9]. The global maxima are connected by almost straight ridges to the “inflection maxima.” As the value of α increases, the height of each ridge decreases towards the limiting value $F=1/4$ (and also the length of each ridge increases) while the line connecting the two saddle points and the minimum approaches the line $u=-v$ with $F=0$. In the (k_x, k_y) plane, the ridges become narrower, higher, and closer together as a function of \mathbf{k} with increasing

TABLE II. Stationary points of $F(u, 0, w)$: Max=maximum, Min=minimum, S = saddle point. See also Fig. 2.

Position (u, w)	No.	F	Value	Type
$\alpha=1$				
(0,0)	1	0	0	Min
$\pm(\sqrt{55/6}/3, 0)$	2	55/168	0.32738	S
$\pm(0, 1/\sqrt{2})$	2	1/4	0.25	S
$\pm(\sqrt{110}/129, \pm\sqrt{5}/43)$	4	100/301	0.33223	Max
$\alpha=2$				
(0,0)	1	0	0	Min
$\pm(\sqrt{7/2}/2, 0)$	2	14/45	0.31111	S
$\pm(0, 1/\sqrt{2})$	2	1/4	0.25	S
$\pm(\sqrt{35}/4, \pm 1/3)$	4	17/54	0.31481	Max

time t . The angle θ between the ridges and the shear direction (k_y direction in this case) is a good measure of theory against experiments because the depth of the temperature quench is unimportant as far as the time dependence is concerned. We find

$$\tan(\theta) = \frac{C_2(\alpha)}{\gamma t}, \quad (19)$$

where $C_2(\alpha)$ is a constant which depends on α , e.g., $C_2(0) = 2(1 - 1/\sqrt{6})$, $C_2(2) = (7 - \sqrt{7})/4$. Equation (19) implies that in the (k_x, k_y) plane, the ridges move closer to the shear direction as time increases. This behavior is found both in simulations [6] and experiments [11].

In the (u, w) plane, there are four maxima, four saddle points, and the global minimum at the origin. These are shown in Table II (for $\alpha=1, 2$), and they can easily be seen in Fig. 2 for $\alpha=1$. When α increases, the peaks and the higher saddle point [i.e., saddle point with higher value of $F(u, 0, w)$] reduce towards the limiting value $F=1/4$ [i.e., $F_m(u, 0, w)$ is deformed towards a ring of radius $1/\sqrt{2}$]. For each value of α , the structure factor pattern in the (k_x, k_z) plane will decrease faster in the flow (i.e., k_x) direction as a function of t , resulting in an elliptical shape with the major

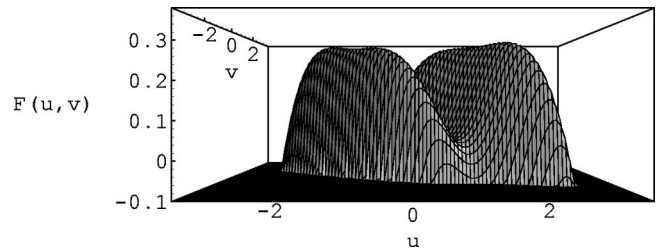


FIG. 1. The graph of $F(u, v, 0)$ for $\alpha=1$. Values for $F(u, v, 0) < -0.1$ are not shown.

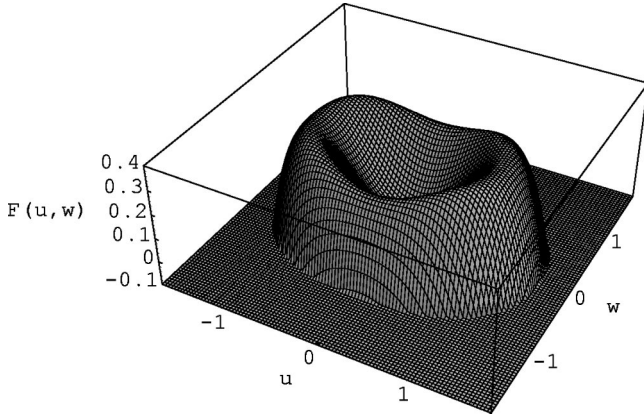


FIG. 2. The graph of $F(u,0,w)$ for $\alpha=1$. Values for $F(u,0,w) < -0.1$ are not shown.

axis along the k_z direction. This elliptical shape has been observed in experiments [11] for scalar fields while the four peaks were not observed.

The excess viscosity $\Delta\eta$, and normal stresses $\Delta N_1, \Delta N_2$ derived by Onuki [2] can be evaluated in the asymptotic limit:

$$\begin{aligned} \Delta\eta &= -(1/\gamma) \int \frac{d^3k}{(2\pi^3)} k_x k_y S(\mathbf{k}, t) \\ &\sim \frac{1}{\gamma^2} \left(\frac{\ln t}{t^{\alpha+3}} \right)^{1/(\alpha+2)}, \\ \Delta N_1 &= \int \frac{d^3k}{(2\pi^3)} (k_y^2 - k_x^2) S(\mathbf{k}, t) \\ &\sim \left(\frac{\ln t}{t} \right)^{1/(\alpha+2)}, \\ \Delta N_2 &= \int \frac{d^3k}{(2\pi^3)} (k_y^2 - k_z^2) S(\mathbf{k}, t) \\ &\sim \left(\frac{\ln t}{t} \right)^{1/(\alpha+2)}. \end{aligned} \quad (20)$$

Numerical calculations [22] show that both excess viscosity $\Delta\eta(t)$ and the normal stress $\Delta N_1(t)$ reach a peak before the asymptotic scaling result. It is not possible to realize this effect as our calculations are strictly valid in the asymptotic regime.

In analogy to 2D numerical calculations presented in [22], it is easy to repeat the calculation for 2D in the shear-flow (k_x, k_y) plane. The self-consistent equation for $a(t)$ leads to [with $C_3(\alpha)$ constant]

$$1 = \frac{C_3(\alpha)\Delta}{\gamma t p_0} \exp\left(2 \frac{p_0^2}{b_0} F_m^{2D}(\alpha)\right), \quad (21)$$

from which to leading order in t ,

$$b_0(t) \approx \left(\frac{\alpha+2}{2} t \right)^{2/(2+\alpha)} \left(\frac{2 \ln t}{\alpha+2} \left[\frac{\alpha+2}{16F_m^{2D}} + \frac{1}{16F_m^{2D}} \right] \right)^{\alpha/(\alpha+2)},$$

$$\frac{p_0^2(t)}{b_0(t)} \approx \frac{\ln t}{2F_m^{2D}} \left[1 + \frac{1}{(\alpha+2)} \right], \quad (22)$$

$$a(t) \approx \left(\frac{4}{(\alpha+2)^2} \frac{\ln t}{t} \right)^{1/(2+\alpha)} \left[\frac{\alpha+2}{16F_m^{2D}} + \frac{1}{16F_m^{2D}} \right]^{1/(\alpha+2)}.$$

Using both Eqs. (21) and (22), the structure factor can be written down as $S(\mathbf{k}, t) = \text{const}(\ln A_s) A_s^{F^{2D}(\mathbf{q})/F_m^{2D}}$, where $A_s = L_x L_y$ is the ‘‘scale area’’ and $\mathbf{q} = (k_x L_x, k_y L_y)$ with $L_x \sim \gamma(t^{5+2\alpha}/\ln t)^{1/2(\alpha+2)}$, $L_y \sim (t/\ln t)^{1/2(\alpha+2)}$, and $F^{2D} = F(u, v, 0)$. Therefore, the structure factor pattern is similar to Fig. 1. The oscillations between the peaks [22] which terminate the two parallel ridges, we believe, are suppressed in the long time regime (i.e., they are the preasymptotic decaying transients).

V. SUMMARY AND REMARKS

We have analytically studied the effect of both shear and order-parameter-dependent mobility on phase separation within the large- n limit. Shear introduces anisotropy in the structure factor pattern because of different growth rates in the flow direction and directions perpendicular to flow. At fixed time t and \mathbf{k} , α distorts the shape of the structure factor $S(\mathbf{k}, t)$ [this is evident in the $F(u, v, 0)$ and $F(u, 0, w)$ patterns]. Similar to all studies previously done, the order-parameter-dependent mobility slows down the rate of coarsening [i.e., $L_i(\alpha=0) > L_i(\alpha \neq 0)$, where $i=x, y, z$]. We believe the multiscaling found here to be the result of the large- n approximation, and that for any finite n , standard scaling will be obtained with the same characteristic length scales but without the $\ln t$ terms, $L_x \sim t^{(2\alpha+5)/2(\alpha+2)}$, $L_y \sim t^{1/2(\alpha+2)}$, and $L_z \sim t^{1/2(\alpha+2)}$. The excess viscosity $\Delta\eta(t)$ and the normal stresses [i.e., $\Delta N_1(t)$ and $\Delta N_2(t)$] relax to zero as $(\ln t/t^{\alpha+3})^{1/(\alpha+2)}$ and $(\ln t/t^{1/(\alpha+2)})$, respectively, in the scaling limit. Again we expect logarithmic terms to be absent for finite n .

ACKNOWLEDGMENTS

N.R. thanks A. Bray for suggesting this problem, and for discussions. N.R. would like to thank Commonwealth Scholarship Commission for financial support.

[1] A.J. Bray, Adv. Phys. **43**, 357 (1994).

[2] A. Onuki, J. Phys.: Condens. Matter **9**, 6119 (1997), and references therein.

[3] D.H. Rothman, Phys. Rev. Lett. **65**, 3305 (1990).

[4] P. Padilla and S. Toxvaerd, J. Chem. Phys. **106**, 2342 (1997).

[5] A.J. Wagner and J.M. Yeomans, Phys. Rev. E **59**, 4366 (1999).

[6] F. Corberi, G. Gonnella, and A. Lamura, Phys. Rev. Lett. (to

- be published); e-print cond-mat/9904423.
- [7] N.P. Rapapa and A.J. Bray, Phys. Rev. Lett. (to be published); e-print cond-mat/9904396.
- [8] F. Corberi, G. Gonnella, and A. Lamura, Phys. Rev. Lett. **81**, 3852 (1998).
- [9] C.K. Chan, F. Perrot, and D. Beysens, Phys. Rev. A **43**, 1826 (1991).
- [10] T. Hashimoto, K. Matsuzaka, E. Moses, and A. Onuki, Phys. Rev. Lett. **74**, 126 (1995).
- [11] J. Lauger, C. Laubner, and W. Gronski, Phys. Rev. Lett. **75**, 3576 (1995).
- [12] J.S. Langer, M. Bar-on, and H.D. Miller, Phys. Rev. A **11**, 1417 (1975); K. Kitahara and M. Imada, Suppl. Prog. Theor. Phys. **64**, 65 (1978).
- [13] D. Jasnow, in *Far from Equilibrium Phase Transitions*, edited by L. Garrido (Springer-Verlag, Berlin, 1988); K. Kitahara, Y. Oono, and D. Jasnow, Mod. Phys. Lett. B **2**, 765 (1988).
- [14] S. Puri, A.J. Bray, and J.L. Lebowitz, Phys. Rev. E **56**, 758 (1997); A.M. Lacasta, A. Hernandez-Machado, J.M. Sacho, and R. Toral Phys. Rev. B **45**, 5276 (1992).
- [15] F. Corberi and C. Castellano, Phys. Rev. E **58**, 4658 (1998).
- [16] A.J. Bray and C.L. Emmott, Phys. Rev. B **52**, R685 (1995).
- [17] C.L. Emmott and A.J. Bray, Phys. Rev. E **59**, 213 (1999).
- [18] R. Ahluwalia, Phys. Rev. E **59**, 263 (1999).
- [19] A. Coniglio and M. Zannetti, Europhys. Lett. **10**, 575 (1989).
- [20] A.J. Bray and K. Humayun, Phys. Rev. Lett. **68**, 1559 (1992).
- [21] A. Coniglio, P. Ruggiero, and M. Zannetti, Phys. Rev. E **50**, 1046 (1994); F. Corberi, A. Coniglio, and M. Zannetti, *ibid.* **51**, 5469 (1995); C. Castellano and M. Zannetti, Phys. Rev. Lett. **77**, 2742 (1996); Phys. Rev. E **53**, 1430 (1996); **58**, 5410 (1998).
- [22] G. Gonnella, A. Lamura, and D. Suppa, e-print cond-mat/9904422.